Research Article GU J Sci 37(1): 90-117 (2024) DOI: 10.35378/gujs.1241638

Gazi University

Journal of Science

http://dergipark.gov.tr/gujs

2-(((2,4-Dichlorophenyl)imino)methyl)-3,4-difluorophenol: X-ray, DFT, MEP, HOMO-LUMO, NLO, Hirshfeld Surfaces, ADMET Profiling, Target Identification, Antipsychotic Activity Against Dopamine D2 and Serotonin 5-HT2A Receptors

Songül SAHIN *

Ondokuz Mayis University, Faculty of Sciences, Department of Chemistry, 55139, Samsun, Türkiye

Highlights

- A tetrahalogenated Schiff base was synthesized and characterized.
- FMOs, NLO, and MEP were studied by the DFT method.
- In silico ADMET and target identification studies were performed.
- Antipsychotic efficacy was evaluated by docking studies.

Article Info

Received: 24 Jan 2023
Accepted: 17 Apr 2023

Keywords

Fluorine compound
Chlorine compound
Schiff base
D2 receptor
5-HT2A receptor

Abstract

Halogenated compounds, especially fluorine and chlorine, play a key role in drug development. They account for a large proportion of all approved drug molecules. The importance of these two halogens stems from their remarkable effects on biological activity and pharmacokinetic properties. The study presented here aims to give the results obtained by the DFT methods and *in silico* medicinal evaluations of a newly synthesized small molecule. The small molecule belongs to the Schiff base class of organic compounds and is substituted with halogen atoms. The tetrahalogenated compound (THSB) Schiff base, 2-(((2,4-dichlorophenyl)imino)methyl)-3,4-difluorophenol, was first synthesized via the classical condensation method and then characterized by spectroscopic techniques. The THSB optimized by the B3LYP method was evaluated in terms of geometrical parameters, surface area (MEP and Hirshfeld analysis) and secondary interaction analysis, NLO properties, and electronic properties (HOMO-LUMO and UV-Vis). Second, THSB was evaluated regarding medicinal chemistry, physicochemical and pharmacokinetic properties, and toxicity (ADMET). Then, we comprehensively investigated the potential biological targets of THSB. Using the results of the SwissSimilarity analysis, we investigated the antagonistic effects of THSB against serotonin 5-HT2A and dopamine D2 receptors. Docking results were compared with the known antipsychotics, clozapine and risperidone. THSB showed a higher antagonistic effect than clozapine for the D2 receptor. However, risperidone proved to be the most effective antagonist for both targets. The binding energies of THSB, risperidone, and clozapine were -8.30, -11.84, and -8.07 kcal/mol, respectively, for D2; those of THSB, risperidone, and clozapine were -6.94, -11.47, and -10.10 kcal/mol, respectively, for 5-HT2A.

1. INTRODUCTION

Schiff bases are compounds that containing a C=N double bond and are expressed by the general formula R1R2C=NR3, where the R groups are organic side chains. These classes of organic compounds are also known as azomethines or imines [1] and can be prepared by condensation of a primer amine and an active carbonyl compound (aldehyde or ketone) [2]. Schiff bases are known for a variety of biological and therapeutic properties [3], such as antifungal, anticancer, antibacterial, and antioxidant properties. They are also used as heterogeneous and homogeneous catalysts, dyes, polymers, and metal removal agents in water [4]. Schiff bases have some advantageous properties such as readily available starting materials, easy preparation and modification methods [5].

*e-mail: songul.sahin@omu.edu.tr

Halogen atoms are commonly used as substituents in pharmaceutical science by medicinal and organic chemists. However, the prevalence of halogens in pharmaceutical chemistry is not proportional. Fluorine is by far the spearhead of halogenated drugs. Chlorinated drugs follow in second place. Bromine and iodine atoms are sparse. Statistics on halogenated drugs approved by the FDA between 1988 and 2006 show that fluorine, chlorine, bromine, and iodine account for 57%, 38%, 4%, and 1%, respectively [6]. In addition, organofluorine drugs account for nearly 20-25% of all marketed drugs [7, 8]. This proportion of fluorine is an issue that synthetic chemists should pay special attention to.

Fluorine with its small size and high electronegativity plays an important role in medicinal chemistry. The substitution of a fluorine atom in an organic compound can alter a number of properties of drug candidates compared to nonfluorinated counterparts. In particular, these effects of fluorine relate to physicochemical and pharmacokinetic (ADME) properties. Thanks to the high electronegativity of fluorine, fluorinated compounds exhibit improved chemical or metabolic stability, membrane permeation, enhanced biological activity [9], binding affinity or interactions [9, 10]. Substitution of fluorine compared to hydrogen atom confers the following functions to a molecule: high electronegativity, greater stability, and greater lipophilicity [9]. A fluorine atom can be bonded to a molecule from different positions. However, the largest bonding type of fluorine drugs among Ar-F, Het-F, Ar-CF3, alkyl-CRF and others is registered as Ar-F containing drugs with 45.3% [7].

Dopamine receptors are a member of the G protein-coupled receptor (GPCR) family. They are associated with some psychotic and neurodegenerative disorders, including schizophrenia, depression, Parkinson's disease, and attention-deficit/hyperactivity disorder [11]. Dopamine receptor D2 (D2R) is an important therapeutic target for the development of antipsychotics, including typical and atypical drugs (first- and second-generation) [11] and for treatment of schizophrenia [12, 13]. However, the pathophysiology of schizophrenia is not limited to the dopamine hypothesis, which states an increase in dopamine-dependent neuronal activity, but is also associated with serotonergic, glutamatergic, GABAergic, and cholinergic systems [12, 14]. Serotonin 2 (5-HT2) type receptors are associated with the serotonergic mechanism of schizophrenia [15]. 5-HT2A receptor antagonists can enhance the antipsychotic effect of first- and second-generation antipsychotics and reduce the symptoms of schizophrenia [16]. Atypical antipsychotics have some advantages over typical antipsychotics and work better than them [13, 16]. The action of atypical antipsychotics as multi-receptor antagonists is one of the reasons why they offer more benefits [13]. Indeed, atypical antipsychotics such as clozapine and risperidone antagonize multiple receptors, including 5-HT1A, 5-HT2A, and D2 [8, 10, 12, 13]. Clozapine remains a prototype for atypical antipsychotics [17].

In the current study, we synthesized a chlorine- and fluorine-substituted tetrahalogenated Schiff base (THSB) and characterized it by combining a number of spectroscopic methods. In addition, we have deepened the study to analyze the electrostatic and surface properties, polarizability, and crystal architecture of the compound using DFT calculations. We then performed *in silico* ADMET and target prediction studies. In the last section, we investigated the antagonistic effect of the Schiff base compound against dopamine (D2) and serotonin (5-HT2A) receptors by docking studies. We also performed the docking studies for the antipsychotics clozapine and risperidone to compare the antagonistic potential of the newly synthesized compound.

2. MATERIAL METHOD

2.1. Chemicals

For the synthesis of the Schiff base compound 2,3-difluoro-6-hydroxybenzaldehyde, 2,4-dichloroaniline, and solvents were purchased from commercial suppliers and used without further purification steps.

2.2. Software and Web Tools

All tools used in this study are listed in the following subtitles.

X-ray diffraction

Diffraction data were acquired using a Bruker Apex II Quazar instrument. The SHELXTL package [18] was used to solve and refine the X-ray diffraction data. All non-hydrogen atoms were refined anisotropically. The free publCIF software [19] was used to edit and preview the CIF file. Molecular graphics were created using Mercury [20]. The CheckCIF validation report [21] was provided by the IUCr website, https://checkcif.iucr.org/, by uploading the CIF file of the compound. For more information on the crystallographic data parameters, see the Cambridge Crystallographic Data Center (CCDC) website [22], https://www.ccdc.cam.ac.uk/, where CCDC 2211899 contains the additional crystallographic data for this work.

Spectroscopic analysis

The experimental FTIR spectrum of the title compound was recorded with a Perkin Elmer instrument between 400-4000 cm^{-1} using the ATR technique. The UV-Vis spectrum was recorded with a Thermo Scientific UV-Vis spectrophotometer between 200-800 nm in an ethanol solution at four concentrations ranging from 1.03 x E-04 M to 5.88 x E-05 M. The theoretical FTIR and UV-Vis spectra were calculated at the DFT [23]/B3LYP/6-311 ++ G (d, p) level of theory [24] in the gas phase using the Gaussian 03W program package and the GaussView molecular visualization program [25].

ADMET and target identification

ADMETLab 2 [26] was used for ADME prediction and physicochemical descriptor calculation. SwissADME [27] was used to determine the physicochemical parameters. ProTox- II [28] was used for toxicity endpoint prediction. TargetHunter [29], PPB [30], and SwissSimilarity [31] were used to determine potential biological targets.

Docking studies

PDB [32] provided 3D structures of the dopamine D2 receptor (PDB ID: 6CM4 [33]) and serotonin 5-HT2A receptor (PDB ID: 6A93 [34]) with the antipsychotic risperidone. AutoDock4 and AutoDockTools4 [35] were used for ligand and receptor preparation and docking experiments. PLIP [36] was used to determine complex interactions. Open Babel [37] was used for a file format converter.

Experimental procedure

A mixture of 2,3-difluoro-6-hydroxybenzaldehyde (0.044 mmol) and 2,4-dichloroaniline (0.044 mmol) was dissolved in absolute ethanol (25 mL) (Figure 1). The mixture was refluxed by stirring for 24 hours. After TLC (hexane: ethyl acetate/9:1) showed the completeness of the reaction, the solution cooled slowly to room temperature and remained at this temperature for one week. The crystallization product (tetra-halogenated Schiff base/THSB: 2-(((2,4-dichlorophenyl)imino)methyl)-3,4-difluorophenol) was used for the structural analyses. Melting point: 165-167 °C. Yield: 77% (9.3 mg). $C_{13}H_7Cl_2F_2NO$. Molecular weight: 302.10 g/mol. FTIR (ATR, ν/cm^{-1}): 3141 (Ar OH); 3083 (Ar CH); 2921 (C<u>H</u>=N); 1653 (C=N); 1616, 1583, 1481, 1458 (Ar C=C); 1342 (Ar C-O); 1254, 1195 (Ar C-N), 1105, 1054 (C-C); 950 (Ar F); 801 (Ar Cl) (Figure 2). UV-Vis (EtOH, 5.88 x E-05 M, λmax/nm (logε): 217 (4.14), 250 (4.29), 320 (3.76) (Figure 3 and Figure S1/experimental).

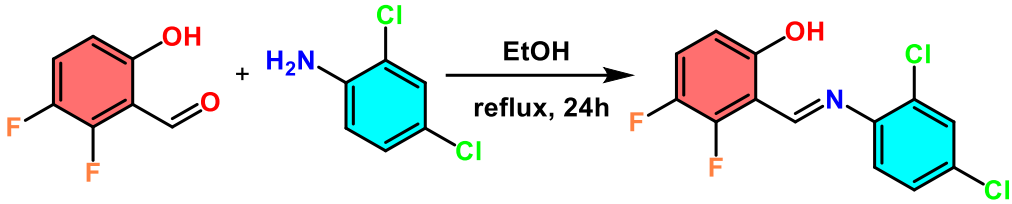

Figure 1. *Synthesis reaction of THSB*

3. THE RESEARCH FINDINGS AND DISCUSSION

3.1. Spectroscopic Evaluations

Using the FTIR spectra of THSB, we determined the functional groups in the molecule. Theoretical (in the gas phase) and experimental (in the solid phase) FTIR spectra of THSB are shown in Figure 2. The main functional groups in the molecule are: Azomethine double bond, azomethine hydrogen, phenolic hydroxyl group, aromatic hydrogens, aromatic double bonds, and aromatic halogen bonds of fluorine and chlorine atoms. The stretching vibration for phenolic hydroxyl occurs at 3141 cm^{-1}. The stretching vibration for aromatic hydrogen atoms is seen at 3083 cm^{-1}. The stretching band of azomethine hydrogen occurs at 2921 cm^{-1}. Azomethine double bond vibrations are observed at 1653 cm^{-1}. Aromatic double bond vibrations occur at 1616, 1583, 1481 and 1458 cm^{-1} as four unique values. The band at 1342 cm^{-1} is assigned to the aromatic carbon-oxygen stretching vibration. The bands at 1254 and 1195 cm^{-1} are evaluated as aromatic carbon-nitrogen bond vibrations. The bands at 1105 and 1054 cm^{-1} are evaluated as single-bond stretching vibrations between aromatic carbon and azomethine carbon. The bands at 950 and 801 cm^{-1} are assigned to the stretching vibrations of fluorine and chlorine, respectively. Visual representations of the experimental and theoretical FTIR spectra of THSB are given in Figure 2. The FTIR spectra of THSB are coherent with each other, with minor deviations due to different molecular interactions in the solid and gas phases.

As an indicator of the electronic transitions in THSB, both the experimental and theoretical UV-Vis spectra are shown in Figure 3 and Figure S1. Experimentally, we observed two absorption maxima at 320 nm and 250 nm, accompanied by a shoulder at 217 nm in ethanol. Theoretically, only one absorption maximum was observed at 347 nm in the gas phase. We evaluated the band at 320 nm as belonging to the $\pi \rightarrow \pi^*$ transition of the azomethine group. The bands at 217 and 250 nm are assigned to the $n \rightarrow \pi^*$ and $\pi \rightarrow \pi^*$ transitions, for which aromatic rings and bound substituents are responsible [38]. The concentration-dependent UV-Vis spectra are shown in Figure 3, indicating the concentrations studied. At higher concentrations, we observed a splitting of the absorption bands and deviations from the Lambert-Beer law due to enhanced molecular interactions.

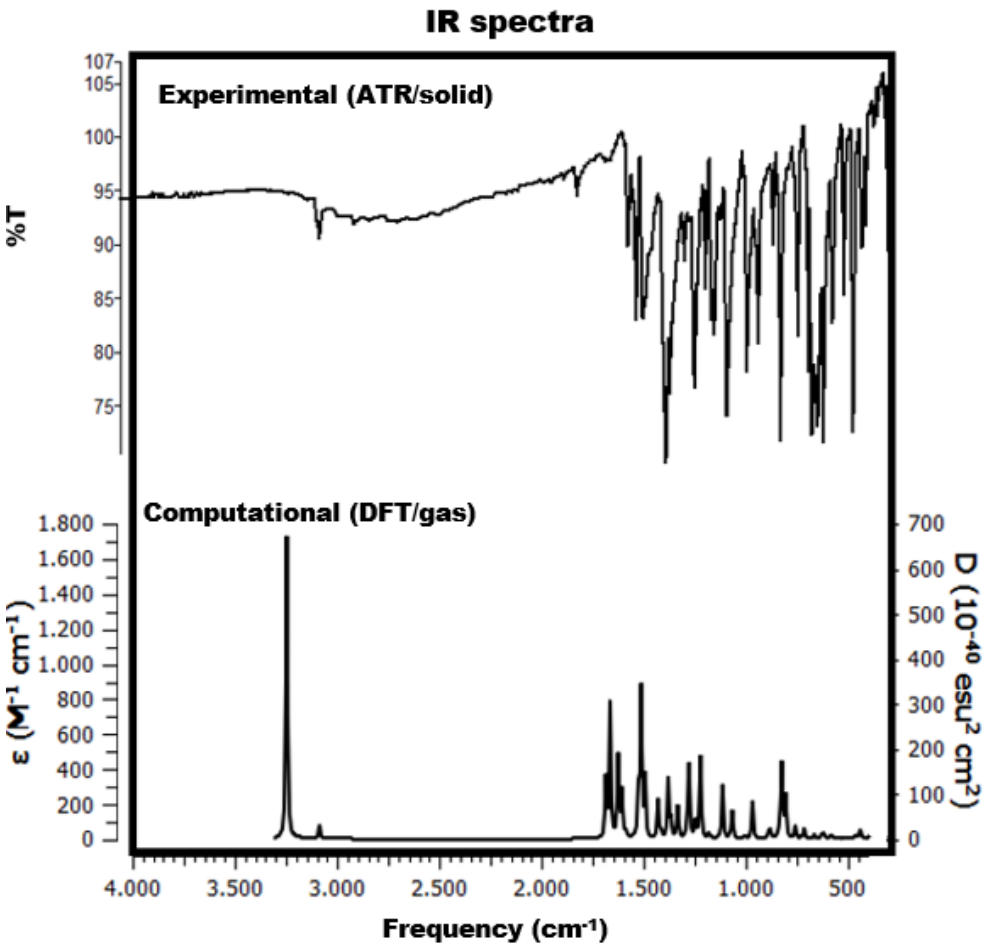

Figure 2. *Comparative (experimental and computational) IR spectra of THSB*

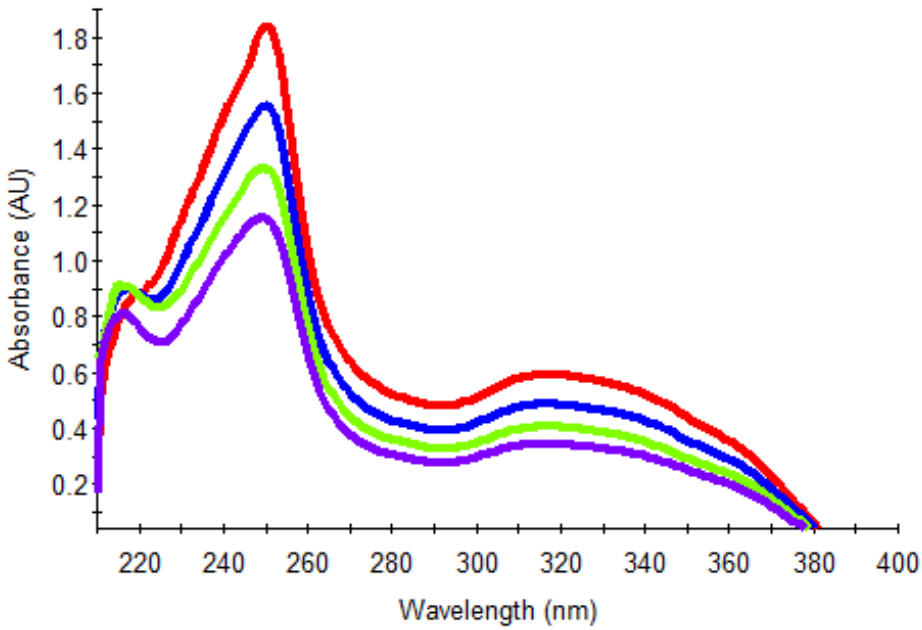

Figure 3. *Experimental UV-Vis spectra of THSB in ethanol at 1.03 x E-04 (red), 8.2 x E-05 (blue), 6.89 x E-05 (green), and 5.88 x E-05 M (purple) concentrations*

3.2. X-ray Analysis and Structural Properties

Suitable crystals for X-ray analysis of THSB were crystallized from absolute ethanol. A crystal with dimensions 0.20 x 0.10 x 0.07 mm^3 was used for data collection. THSB has a monoclinic crystal system ($\alpha = \gamma \neq \beta$; 90°, 90°, 98.90° : $a \neq b \neq c$; 16.102 (5) Å, 3.7816 (11) Å, 20.481 (6) Å) and a space group P21/n. The other crystal data, data collection and refinement parameters are listed in Table S1. The experimental and computational geometrical parameters including bond lengths, bond angles, and torsions for THSB are listed in Table S2, Table S3, and Table S4, respectively. The unit cell plot (Z=4) and ORTEP structure with a probability level of 50% for THSB are shown in Figure 4. In the bottom right of Figure 4, we have shown intermolecular secondary interaction points in the THSM and indicated the interacting atoms (F2, Cl2, O1, H5, H3) along with the bond lengths. We have also included the list of hydrogen bonds in the molecule in Table 1. From the Figure 4 and Table 1, we can see that molecular assembly is predominantly stabilized by two intermolecular (H3---O1/2.46 Å and H5---N2/2.61 Å) and one intramolecular (H2---N1/1.88 Å) hydrogen bonds. We see the same interacting atoms in Figure 6, which shows dnorm plots on the Hirshfeld surface of THSB with different positions. Deep and dim red dots on the Hirshfeld surface represent strong and weak interaction sites in a molecule [39]. On this surface (Figure 6), deep reds are on atoms O1 and H3, the others are dim red and are on atoms F2, Cl2, and H5 of the molecule (see Figure S2 for high resolution). The strongest hydrogen bonding in Table 1 is indicated between atoms O1 and H3 for intermolecular interactions, and this strongest interaction was also doubly confirmed by the deepest red dots on the Hirshfeld surface. The other Hirshfeld surfaces, including shape index, di, de, dnorm, curvedness, and fragment patch are shown in Figure 5. Adjacent blue-red triangles in the shape index map and flat surfaces in the curvedness map show the presence of π-π type interaction (π-π stacking) [40] established between aromatic rings. We have also investigated the contribution of individual atoms to all non-covalent interactions in Figure 7 using the fingerprint analysis of CrystalExplorer [41]. The largest contribution belongs to the H interactions with 45.8%. This is followed by the interactions between C and other atoms with 18.7%. The others are as follows: Cl 15.7%, F 14%, O 4.2%, and N 1.6%. All the above interactions show a crystalline architecture and crystal lattice as shown in Figure 8 for THSB.

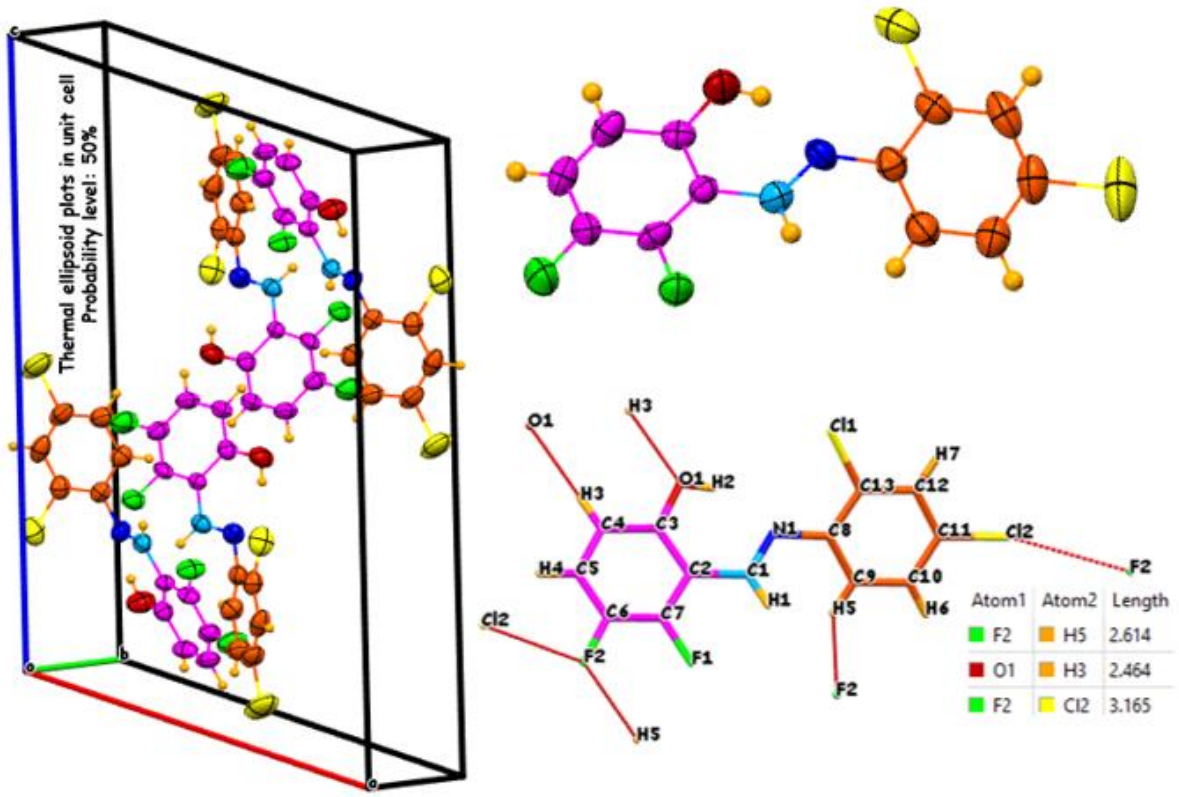

Figure 4. *A unit cell view of THSB (left), thermal ellipsoid plot diagram of THSB with a 50% probability level (top right), secondary interaction places of THSB along with interacted atoms and bond lengths (bottom right)*

Table 1. *Hydrogen bong geometry list for THSB*

	Hydrogen-bond geometry (Å, °)			
D—H···A	**D—H**	**H···A**	**D···A**	**D—H···A**
C4—H3···O1^{i}	0.93	2.46	3.375 (4)	166
C9—H5···F2^{ii}	0.93	2.61	3.345 (4)	136
O1—H2···N1	0.80 (3)	1.88 (3)	2.589 (4)	147 (4)

Symmetry codes: (i) -x+1, -y+2, -z+1; (ii) -x+1/2, y+1/2, -z+1/2.

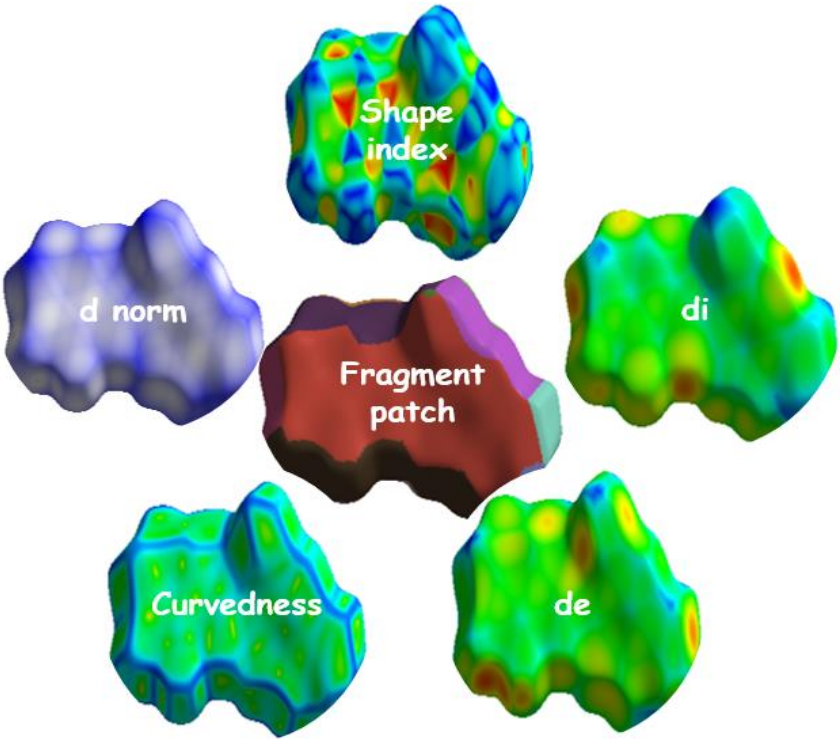

Figure 5. *Hirshfeld surfaces mapped with shape index, di, de, curvedness, dnorm and fragment patch for THSB*

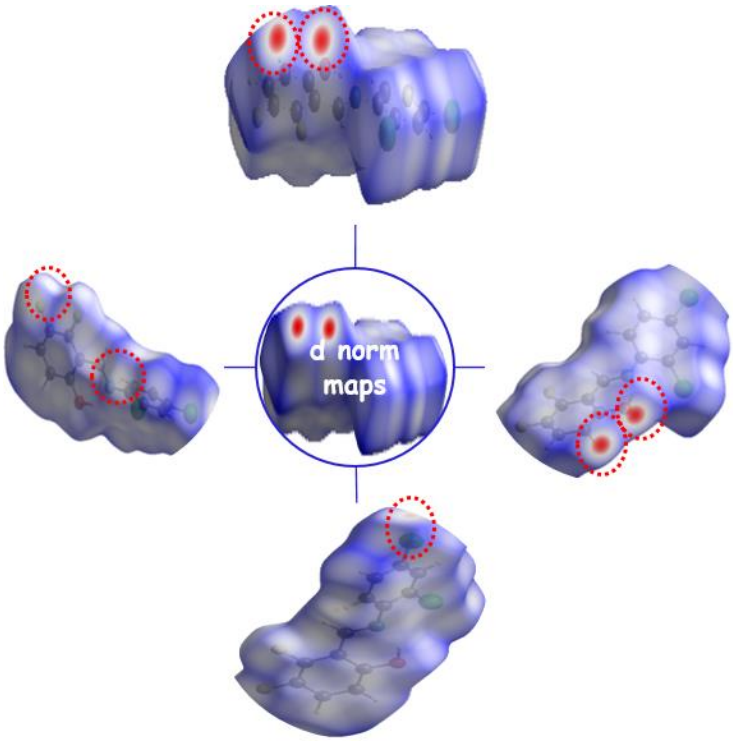

Figure 6. *Views of dnorm surface from different positions, small and big red dots sign out molecular interaction places (on the O1, Cl2, F2, H3, H5 atoms)*

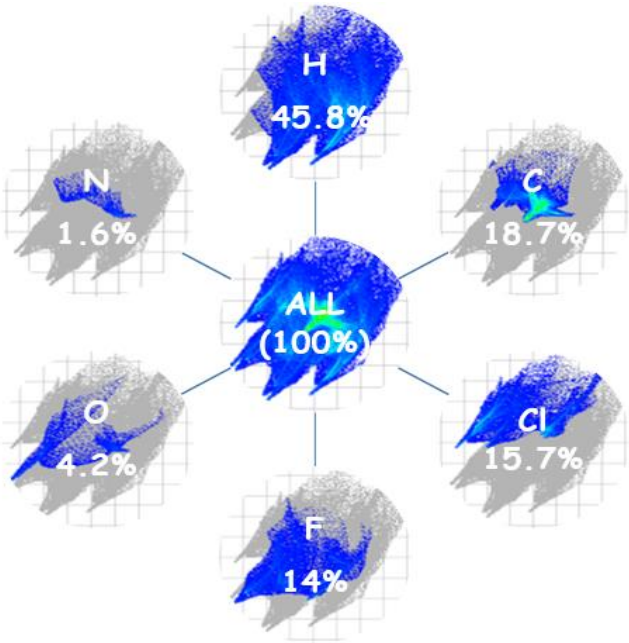

Figure 7. *The contribution percentage to whole intermolecular interactions per each atom*

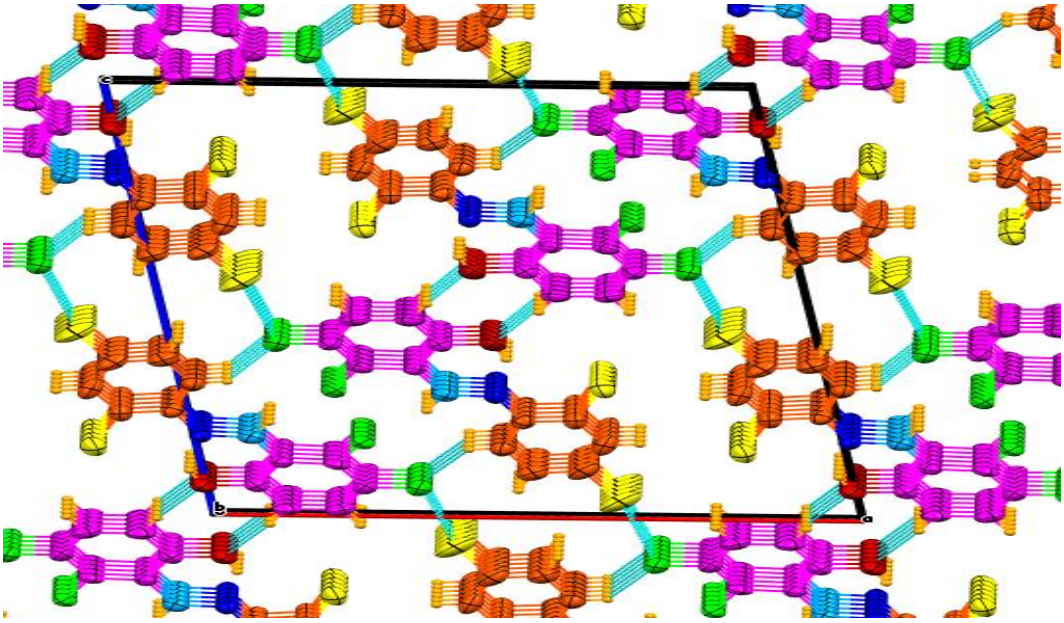

Figure 8. *A section from the crystalline arrangement of THSB*

3.3. DFT Studies

In this section, we carried out all calculations using the Gaussian 03W and GaussView program packages. Geometry optimization, frequency and energy calculations were performed using the B3LYP method and the 6-311 ++ G (d, p) basis set. The other settings were kept in the default mode of the program.

Molecular electrostatic potential (MEP) map

The MEP surface of THSB is provided in Figure 9. The color codes change in the range of -4.478 x E-02 and 4.478 x E-02. The negative and positive extreme points in this map show the deepest red and deepest blue regions, respectively. In this map, colors changes according to the electron density of the molecule, and the regions with high electron density and low electron density are colored red and blue, respectively.

The regions between red and blue indicate neutral regions. In this way, reactive regions of a molecule, intermolecular interaction points, and electrophilic and nucleophilic attack regions can be determined by means of the MEP map [42]. In Figure 9, the reddish-yellow region is spread over the phenolic oxygen atom (O1), and this atom can act as a hydrogen acceptor or electrophilic attack center in any possible intermolecular interactions or reactions. The blue regions are spread over the H1, H3, H4, and H5 atoms, and these atoms can involve in hydrogen bond formations or act as nucleophilic attack centers. We have already seen the atoms O1, H3, and H5 in the intermolecular interactions for the mentioned roles above.

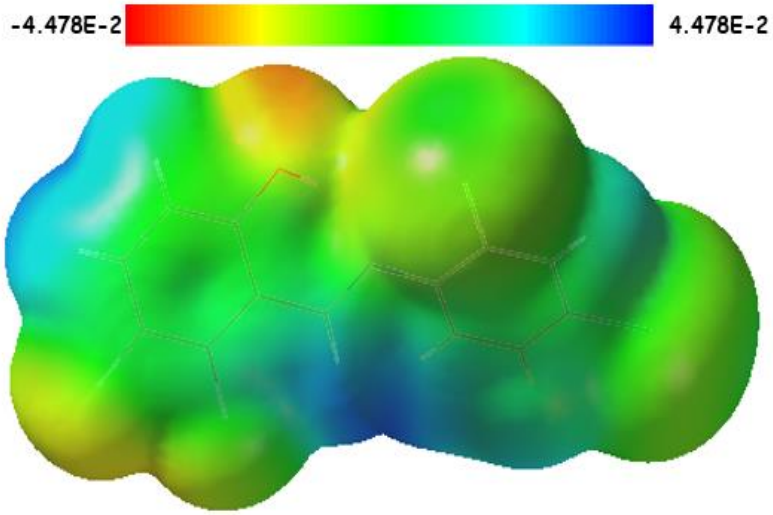

Figure 9. *Molecular electrostatic potential map of THSB*

Frontier molecular orbitals (FMOs) and energy gap

The highest occupied molecular orbital and the lowest unoccupied molecular orbital, also known as HOMO and LUMO orbitals or frontier molecular orbitals, determine the ability to donate and accept electrons between the ground and excited states of a molecule. These orbitals and their energy gap (ΔE) are a useful method for determining chemical reactivity, kinetic stability, polarizability, and predicting the softness and hardness of a molecule [43]. Figure 10 shows a pictorial representation of the HOMO and LUMO orbitals. The HOMO, LUMO, and HOMO-LUMO gap energies for THSB are -6.7239, -2.55483, and 4.1756 eV, respectively, as shown in Figure 10. The HOMO and LUMO orbitals are localized throughout the molecule and show charge delocalization within THSB. From the energies of these orbitals, we also calculated the FMO parameters (global reactivity descriptors), as indicated in Table 2. The ionization potential (I=-EHOMO) and electron affinity (A=-ELUMO) depend directly on the energies of the HOMO and LUMO orbitals and are calculated to be 4.1756 and 6.7239 eV for THSB, respectively. The chemical hardness (μ=(I-A)/2) and softness (S=1/2η) determine the reactivity of a molecule [44]. They are related to the energy of the band gap between HOMO and LUMO orbitals, and hard and soft molecules have large and small energy gaps, respectively [45]. Chemical hardness provides information about an atom's resistance to charge transfer, while softness is a measure of an atom's ability to accept electrons [46]. A hard molecule expresses low reactivity, high chemical stability, and low polarizability, while a soft molecule means the opposite. The calculated values of chemical hardness and softness for THSB are 2.0378 and 0.2390, respectively. The electronegativity (χ=(I+A)/2) is a measure of the electron attraction capacity of the molecules and was calculated to be 4.6361 for THSB. The electrophilicity index ($\omega = \mu^2/2\eta$) is defined as the energy change of an electrophilic species when it reacts with a strong nucleophile, or the stabilization energy gained when the system is saturated with electrons, and it is used to predict biological activity [46]. The calculated value of ω is 5.1473. Good nucleophilic and electrophilic species are characterized by low and high values of μ and ω, respectively [47]. The chemical potential (μ =-(I+A)/2) for THSB was calculated to be -4.6361. The energy gap value of THSM (4.1756) is not an extreme value to compare, as different groups have reported lower [46, 48, 49] and higher [45, 50] energy gap values. Therefore, we

cannot draw concrete conclusions and say that the THSM is stable or not stable, polarizable or not polarizable, chemically reactive or not reactive, biologically active or not active. For an accurate comparison, we should have comparable molecules that differ only slightly.

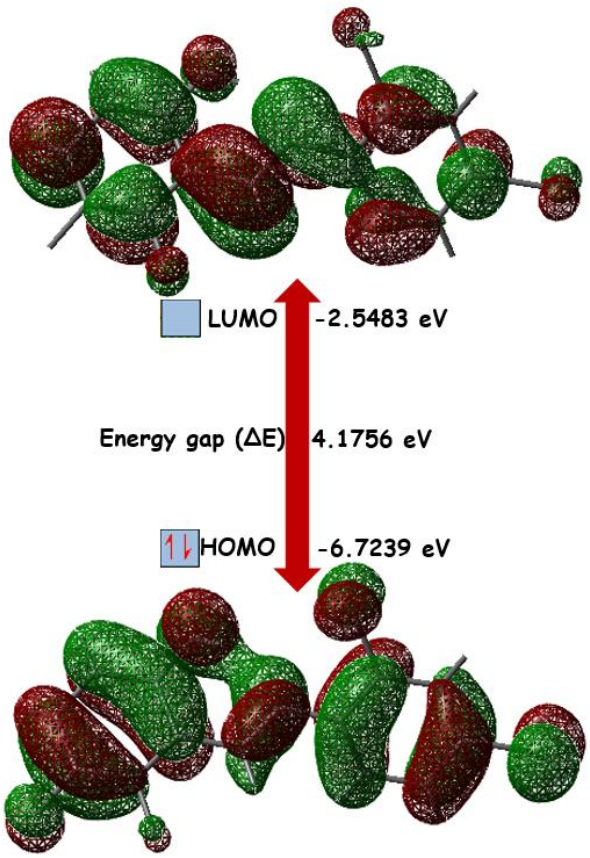

Figure 10. *HOMO and LUMO orbitals of THSB*

Table 2. *Chemical reactivity descriptors of THSB*

Parameters	**Value (eV)**
E_{HOMO}	-6.7239
E_{LUMO}	-2.5483
Energy band gap ($\Delta E = E_{LUMO}-E_{HOMO}$)	4.1756
Ionization potential ($I = -E_{HOMO}$)	6.7239
Electron affinity ($A = -E_{LUMO}$)	2.5483
Chemical hardness ($\eta = (I-A)/2$)	2.0878
Chemical softness ($S = 1/2\eta$)	0.2390
Electronegativity ($\chi = (I+A)/2$)	4.6361
Chemical potential ($\mu = -(I+A)/2$)	-4.6361
Electrophilicity index ($\omega = \mu^2/2\eta$)	5.1473
Maximum charge transfer index ($\Delta n_{max} = -\mu/\eta$)	2.2205

Non-linear optic (NLO) properties

The values for the mean dipole moment (μ), isotropic mean polarizability (α_{iso}), anisotropic polarizability (α_{aniso}), and mean first-order hyperpolarizability (β_{tot}) for THSB are shown in Table 3. In this table, the NLO parameters were calculated using the x, y, and z components of THSB. These calculations were

performed to the equations given in [51]. An NLO active molecule is a one that has easily polarizable electrons and generally consists of three components, including a donor group, an acceptor group, and a conjugated bridge [52].

Since the Gaussian output file gives the results in atomic units (a.u.), the final values were converted to esu units using the equations in Table 3. The mean dipole moment (μ) was determined to be 1.1226 D, and mean isotropic (α_{iso}) and anisotropic polarizability (α_{aniso}) were calculated to be 9.2788 x 10^{-26} and 4.5341x10^{-23} esu, respectively. The value of first order hyperpolarizability (β_{tot}) were determined as 0.9476x10^{-30} esu. Urea, also known as carbamide, is used as a prototype for evaluating the hyperpolarizability properties of the studied compound and for comparative purposes [51]. The mean dipole moment of THSB is smaller than that of urea (0.8175-fold), but the first-order hyperpolarizability, an important parameter for the high NLO capacity of THSB, is 2.5411-fold larger than that of the standard molecule urea. Therefore, THSM can be considered as a candidate NLO material.

Table 3. *Calculated values of mean dipole moment, mean iso/aniso polarizability, and first-order hyperpolarizability and their computational components*

Parameters	B3LYP	Parameters	B3LYP	Parameters	B3LYP
μ		**α**		**β**	
μ_x	-0.4409	α_{xx}	-122.8121	β_{xxx}	-96.7163
μ_y	-0.8466	α_{yy}	-122.9734	β_{yyy}	-22.7344
μ_z	-0.5908	α_{zz}	-123.3726	β_{zzz}	10.7546
μ (Debye)	1.1226	α_{xy}	-7.5902	β_{xyy}	6.1558
μ_{urea} [53]	1.3732	α_{xz}	2.2006	β_{xxy}	57.3448
μ/μ_{urea}	0.8175	α_{yz}	3.0944	β_{xxz}	-10.3128
		α_{iso} (a.u.)	-0.6261	β_{xzz}	-13.1156
		α_{aniso} (a.u.)	305.9467	β_{yzz}	-7.4725
		α_{iso} (esu)	9.2788x10^{-26}	β_{yyz}	-3.2122
		α_{aniso} (esu)	4.5341x10^{-23}	β_{xyz}	3.2985
				β (a.u.)	107.2048
				β_{tot} (esu)	0.9476x10^{-30}
				β_{urea} (esu) [51, 53]	0.37289x10^{-30}
				β_{tot}/β_{urea}	2.5411

1 a.u. = 0.1482 × 10^{-24} esu for α; 1 a.u. = 0.0088393 × 10^{-30} esu for β [54]

3.4. Physicochemical Descriptors for Medicinal Chemistry

The physicochemical properties of THSB were listed in Table 4 to show the deviations from the idealized properties according to the online platforms ADMETLab. 2 and SwissADME. Appropriate limits for the oral bioavailability of a chemical substance are available for both ADMETLab and SwissADME algorithms, and the corresponding radar plots are shown for THSB in Table 4. ADMETLab 2.0 and SwissADME show the ideal ranges with mustard and pink colors, respectively. The properties of our compound are shown with a blue line in the ADMETLab.2 diagram, and with a red line in the SwissADME diagram.

In the ADMETLab 2.0 results, among the investigated physicochemical parameters (molecular weight, volume, nHA, nHD, nRot, nRing, nRig, nHet, fChar, TPSA, logS, logP, logD7.4), logD, logS and logP show deviations from the acceptable range. LogP and logD deviate from maximum, while LogS deviates from minimum. These parameters indicate the logarithm of water solubility (logS), the n-octanol/water partition coefficient (logP), and the n-octanol/water partition coefficient at pH=7.4 (logD7.4). They are important for oral absorption, membrane permeability, hydrophilic bonding, dissolution in body fluid, and biomembrane penetration. Hence, it is necessary to consider them at the beginning of the drug development stages. A suitable range for LogP, LogD, and LogD is 0-3 logmol/L, 1-3 logmol/L, and (-4)-0.5 logmol/L, respectively. The values calculated of these parameters for THSB are 4.784, 3.976, and -5.75, respectively.

In the SwissADME results, among the six parameters studied, lipophilicity (LIPO), size, polarity (POLAR), insolubility (INSATU), insaturation (INSATU), and flexibility (FLEX), the INSATU value is outside the appropriate range. The ideal INSATU value is between 0.25 and 1.0 (0.25<fraction Csp3<1). The calculated value of INSATU for THSB is 0.00.

Table 4. *Physicochemical properties of the compound THSB calculated by two web-servers*

Physicochemical Properties	**ADMETLab 2.0**	**SwissADME**
Main property chart	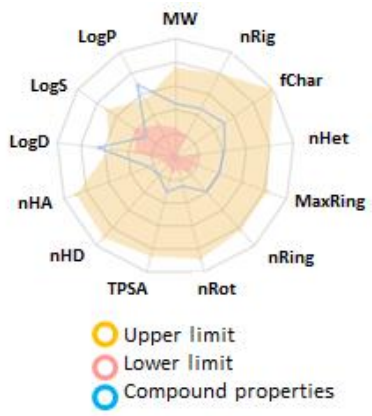	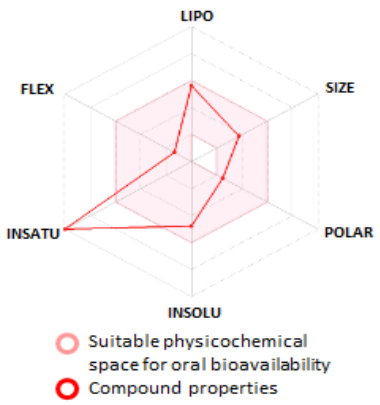
Input	OC1=CC=C(F)C(F)=C1\C=N\C1=CC=C(Cl)C=C1Cl	
Formula	Nr (Not reported)	$C_{13}H_7Cl_2F_2NO$
Molecular weight	300.99	302.10
Heavy atoms	Nr	19
Aromatic heavy atoms	Nr	12
Fraction Csp^3	Nr	0
Number rotatable bonds	2	2
Hydrogen bond acceptors	2	4
Hydrogen bond donors	1	1
Molar refractivity	Nr	72.10
TPSA (Å^2)	32.590	32.59
logS	-5.75	-4.77 (poorly soluble)
$LogP_{(o/w)}$	4.784	4.47
logD (logP at phys. pH)	3.976	Nr
nRing	2	Nr
MaxRing	2	Nr
nHet	6	Nr
fChar	0	Nr
nRig	13	Nr
Flexibility	0.154	Nr
Stereo Centers	0	Nr

3.5. In silico ADMET Analysis

One of the major obstacles in drug development is poor pharmacokinetic properties. This is followed by low efficacy and toxicity [55]. Pharmacokinetics includes the absorption, distribution, metabolism, and excretion (ADME) of a drug in the body. Early ADMET profiling is necessary to avoid the time-consuming process, high cost, and waste of resources. Various *in silico* tools have been developed for this purpose [56]. Some medicinal chemistry and ADME endpoints for THSB are listed in Table 5. In this table, the red circle indicates poor pharmacokinetic properties, and the green circle indicates that the endpoint meets the accepted requirements of the domain. Table 5 shows that THSB deviates from Fsp3, MCE-18, Pfizer, and GSK rules. Fsp^3 is the number of saturated carbon atoms compared to the whole molecule, and the ideal range for this value is greater than or equal to 0.42 ($Fsp^3 \geq 0.42$/excellent). MCE-18 is a measure of the

effective value, novelty, and lead potential of a molecule. It can be calculated by a combination of aromaticity, non-aromaticity, chirality, spiro value, and quadratic index. If the values of MCE-18 are greater than or equal to 45, the molecule is classified as "excellent." The calculated value for THSB is 13.00 and is classified as insufficient. The Lipinski rule refers to absorption or permeability [57], while the Pfizer rule refers to toxicity [58]. In the Pfizer rule, there is an analogy for toxicity between low polarity and high lipophilicity. A high logP value (> 3) and a low TPSA value (< 75) of a compound are likely to be associated with increased toxicity. The calculated values of logP and TPSA or THSB are 4.784 and 32.59 (ADMETLab. 2.0), so THSB could be a toxic compound. The GSK rule emphasizes that the improvement of desired ADMET results is more possible with low values of logP (≤ 4) and molecular weight (≤ 400) [59], and 0 violations of the GSK rule are considered excellent. The found value of logP for THSB is 4.784, and therefore it is not classified in the green range.

For the ADME parameters, there are no violations of the adsorption endpoints, and most of them are classified as green. The distribution endpoint Fu, the unbound fraction of a drug in plasma, does not represent a good value for THSB. The calculated clearance rate (CL) is 1.917 ml/min/kg, and İT is considered a poor value. The optimal threshold for CL is more than 5 ml/min/kg [26].

THSB exhibits some toxic activities related to the mitochondrial membrane potential (MMP) and aryl hydrocarbon receptor (AhR). In addition, the compound was found to be moderately toxic in terms of carcinogenicity and mutagenicity (Table S5), which is consistent with the Pfizer rule mentioned above.

Table 5. *Medicinal chemistry and ADME predictions according to the ADMETLab 2.0*

Medicinal Chemistry	**ADMETLab 2.0**	**Indicator**	**Prediction probability**
QED	0.799	🟢	
SAscore	2.530	🟢	
Fsp^3	0.000	🔴	
MCE-18	13.000	🔴	
NPscore	-1.430		
Lipinski rule	Accepted	🟢	
Pfizer rule	Rejected	🔴	
GSK rule	Rejected	🔴	
Golden triangle	Accepted	🟢	
PAINS	0 alert		
Alarm NMR rule	2 alerts		
BMS rule	0 alert		
Chelator rule	0 alert		
Absorption		🟢	
Papp (Caco-2 permeability)	-4.864	🟢	
MDCK permeability	1.2xE-05	🟢	
Pgp-inhibitor	0.039	🟢	---
Pgp-substrate	0.001	🟢	---
HIA (Human intestinal absorption)	0.003	🟢	---
F (30% Bioavailability)	0.001	🟢	---
F (20% Bioavailability)	0.431	🟡	-
Distribution			
PPB (Plasma protein binding)	100.3%		
VD (Volume distribution)	1.236	🟢	
BBB penetration (Blood-brain barrier)	0.445	🟡	-
Fu	0.822%	🔴	
Metabolism			
CYP1A2 inhibitor	0.966		+++
CYP2C19 inhibitor	0.848		++
CYP2C9 inhibitor	0.643		+
CYP2D6 inhibitor	0.65		+
CYP3A4 inhibitor	0.107		--
CYP1A2 substrate	0.61		+
CYP2C19 substrate	0.084		---
CYP2C9 substrate	0916		+++
CYP2D6 substrate	0.798		++
CYP3A4 substrate	0.177		--
Excretion			
$T_{1/2}$ (Half life time)	0.061 h (short)		-
CL (Clearance rate, ml/min/kg)	1.917 (low)	🔴	

Tips: For the classification endpoints, the prediction probability values are transformed into six symbols:

0-0.1(---), 0.1-0.3(--), 0.3-0.5(-), 0.5-0.7(+), 0.7-0.9(++), and 0.9-1.0(+++).

🔴 poor; 🟢 excellent; 🟡 medium

3.6. Identification of Biological Targets

To identify potential biological targets of THSB, we performed ligand-based screening across platforms based on molecular fingerprints using several web tools, including Polypharmacology Browser 2 (PPB2), TargetHunter, and SwissSimilarity web tools. These tools use single or multiple fingerprint algorithms or sometimes their combinations (Tables 6 and 8), to predict potential targets for the compounds under investigation by loading SMILES or 2D structures of small molecules. We used the multiple fingerprint and combination methods of PPB 2 and SwissSimilarity, and path-based fingerprint method (FP2) of TargetHunter for the search. In PPB2 and TargetHunter, the entire ChEMBL database was selected as the ligand screening library, and in SwissSimilarity, the ChEMBL-approved drug database was selected. The results of PPB2 are presented in Table 6 by listing the first twenty results. The results of TargetHunter are presented in Table 7 by listing the first ten results. For the SwissSimilarity platform, we reported the search parameters in Table 8 and listed the first two results (Table 9) with the highest similarity score. For the molecular docking studies, we adopted the results from the database of approved drugs (SwissSimilarity platform), as they are fully approved drugs.

PPB 2 and Target Hunter together revealed that THSB is effective as an antagonist against the bacteria Pseudomonas fluorescents, Escherichia coli, and Staphylococcus aureus. In addition, PPB 2 suggests an inhibitory effect of THSB on these targets: ATPase_family_AAA_domain-containing_protein_5, Plasmodium falciparum guanine_nucleotide-binding_protein_G(s)_subunit_alpha, nuclear_receptor_ROR-gamma, prelamin-A/C, survival_motor_neuron_protein, beta-lactamase_AmpC, 6-phospho-1-fructokinase, ataxin-2, histone-lysine_N-methyltransferase_H3_lysine-9_specific_3, PC-3, hepatitis_C_virus, DNA_polymerase_iota, luciferin_4-monooxygenase, geminin, HCT-116, and U-251 (Table 6). TargetHunter listed very similar compounds (Table 7) that have in vitro results along with their targets. The other potential activities were predicted for Bacillus subtilis, Enterococcus faecalis, Enterococcus faecium, radical scavenging activity, acidic alpha-glucosidase, sentrin-specific protease 1, and beta-amyloid A4 protein.

The SwissSimilarity search was limited to approved drugs, and THSB showed similarity to the approved antipsychotics, loxapine (similarity rate: 0.469) and clozapine (similarity rate: 0.404). The other comparative parameters between the above antipsychotics and THSB are shown in Table 9. Clozapine is an atypical drug (second generation) and has antagonistic effects on both 5-HT2A and D2 receptors [60]. Therefore, due to the moderate similarity between clozapine and THSB, docking experiments were performed on these receptors.

Table 6. *Druggable target list for THSB predicted by Polypharmacology Browser according to various fingerprint methods*

No	ChEMBL Name (ID)	APfp	Xfp	MQN	SMIfp	Sfp	ECfp4	Ffp1	Ffp2	Ffp3	Ffp4	No of mols
1	ATAD5 (1741209)			0.082	0.207	0.188						9
2	ORGANISM (364)			0.069	0.229	0.206	0.069					**20**
3	GNAS (4377)			0.087	0.241	0.231	0.042	0.013	0.021			6
4	RORC (1293231)					0.181	0.034		0.015			4
5	LMNA (1293235)		0.022		0.434	0.196	0.058					4
6	SMN1 (1293232)		0.024	0.401		0.195			0.01			2
7	AMPC (2026)						0.044	0.011	0.021			3
8	PFK (5686)					0.154						1
9	ATXN2 (1795085)		0.034			0.182			0.016	0.011	0.011	2
10	EHMT2 (6032)				0.497	0.138		0.034		0.045	0.037	5
11	CELL-LINE (390)											1
12	ORGANISM (379)			0.015		0.031						1
13	POLI (5391)					0.129		0.03		0.043	0.034	2
14	ORGANISM (612500)											3
15	NA (5567)			0.195	0.343		0.038					8
16	GMNN (1293278)			0.178	0.229	0.219						4
17	ORGANISM (352)											1
18	ORGANISM (354)											2
19	CELL-LINE (394)											1
20	CELL-LINE (615022)											1

Color indicator Target not found | p-value > 0.01 | p-value (0.01-0) | Number of similar molecules

Instructions:

1 ATPase_family_AAA_domain-containing_protein_5
2 Plasmodium falciparum
3 Guanine_nucleotide-binding_protein_G(s)_subunit_alpha
4 Nuclear_receptor_ROR-gamma
5 Prelamin-A/C
6 Survival_motor_neuron_protein
7 Beta-lactamase_AmpC
8 6-phospho-1-fructokinase
9 Ataxin-2
10 Histone-lysine_N-methyltransferase_H3_lysine-9_specific_3
11 PC-3
12 Hepatitis_C_virus
13 DNA_polymerase_iota
14 Pseudomonas fluorescens
15 Luciferin_4-monooxygenase
16 Geminin;
17 Staphylococcus aureus
18 Escherichia coli
19 HCT-116
20 U-251

Table 7. *Similar structure list to THSB for top ten compounds from ChEMBL database and their bioactivity. The results were retrieved from Target Hunter and listed to path-based fingerprints (FP2)*

No	Similar structures	Similarity score	Target	Bioactivity type	Value	Ref.
1	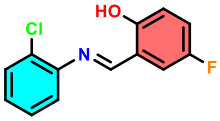 ChEMBL1241109	0.88	**Pseudomonas fluorescens** **Escherichia coli** Bacillus subtilis **Staphylococcus aureus**	Activity	12.5 µg ml^{-1} 6.25 µg ml^{-1} 12.5 µg ml^{-1} 12.5 µg ml^{-1}	[61]
2	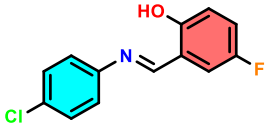 ChEMBL1241042	0.85	Pseudomonas fluorescens Escherichia coli Bacillus subtilis Staphylococcus aureus	Activity	25 µg ml^{-1} 12.5 µg ml^{-1} 50 µg ml^{-1} 25 µg ml^{-1}	
3	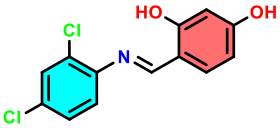 ChEMBL1928487	0.75	Escherichia coli Enterococcus faecalis Enterococcus faecium Staphylococcus aureus Staphylococcus aureus	MIC	64 µg ml^{-1} >512 µg ml^{-1} >512 µg ml^{-1} 128 µg ml^{-1} 128 µg ml^{-1}	[29]
4	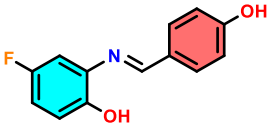 ChEMBL1241044	0.72	Pseudomonas fluorescens Escherichia coli Bacillus subtilis Staphylococcus aureus	Activity	>100 µg ml^{-1} >100 µg ml^{-1} >100 µg ml^{-1} 12.5 µg ml^{-1}	
5	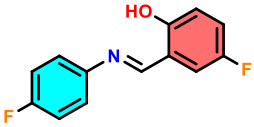 ChEMBL1240984	0.72	Pseudomonas fluorescens Escherichia coli Bacillus subtilis Staphylococcus aureus	Activity	12.5 µg ml^{-1} 12.5 µg ml^{-1} 12.5 µg ml^{-1} 12.5 µg ml^{-1}	[61]
6	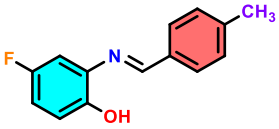 ChEMBL1240982	0.72	Pseudomonas fluorescens Escherichia coli Bacillus subtilis Staphylococcus aureus	Activity	50 µg ml^{-1} 50 µg ml^{-1} >100 µg ml^{-1} 100 µg ml^{-1}	
7	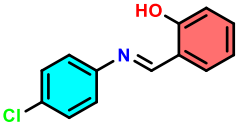 ChEMBL2236402	0.72	Radical scavenging activity Acidic alpha-glucosidase	Activity INH	Not active 5.63%	[62]
8	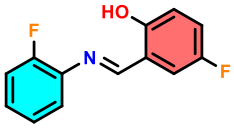 ChEMBL1241108	0.71	Pseudomonas fluorescens Escherichia coli Bacillus subtilis Staphylococcus aureus	Activity	6.25 µg ml^{-1} 6.25 µg ml^{-1} 12.5 µg ml^{-1} 6.25 µg ml^{-1}	[61]
9	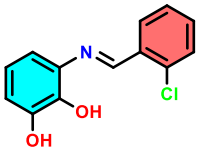 ChEMBL2159849	0.70	Sentrin-specific protease 1	INH	Not active	[63]
10	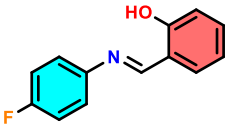 ChEMBL3098347	0.67	Beta amyloid A4 protein Radical scavenging activity	INH IC50	24.9% >1000 µM	[29]

Table 8. *Selection of search parameters for molecular similarity prediction by means of Swiss Similarity*

	2D								3D	2D & 3D
	FP2	ECFP4	MHFP6	Pharmacophore	ErG	Scaffold	Generic Scaffold	Electroshape	E3FP	Combined
DrugBank	○	○	○	○	○	○	○	○	○	○
ChEMBL approved drugs	○	○	○	○	○	○	○	○	○	◉
ChEMBL drug candidates in clinics	○	○	○	○	○	○	○	○	○	○

Table 9. *The two drugs similar to THSB with a similarity score of 0.404 and 0.469 from the ChemMBL-approved drugs, and their indications*

	Query compound	**Clozapine**	**Loxapine**
Molecular structure	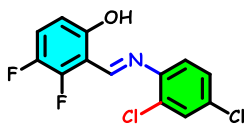	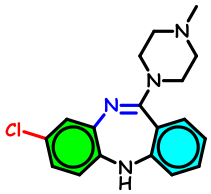	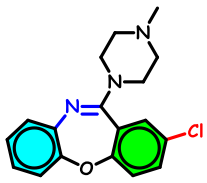
Similarity score		0.404	0.469
ChEMBL code		CHEMBL42	ChEMBL831
Molecular formula	$C_{13}H_7Cl_2F_2NO$	$C_{18}H_{19}ClN_4$	$C_{18}H_{18}ClN_3O$
Molecular weight (g/mol)	302.10	326.83	327.81
Indication		Schizophrenia	Schizophrenia

3.7. Molecular Docking Experiments

We performed molecular docking experiments according to the SwissSimilarity results, which revealed the highest similarity rate between the query compound (THSB) and the antipsychotics clozapine and loxapine. These are very similar drugs, differing only by the bridging atom between the phenyl groups (Table 9). Both are atypical drugs used to treat schizophrenia. Loxapine [64] and clozapine [17] show antagonistic effects on both dopamine D2 receptors and serotonin 5-HT2A receptors. Therefore, we investigated the dual antagonistic effects of THSB on D2 and 5-HT2A receptors by molecular docking experiments. The accessible 3D complex of these receptors is with risperidone, another atypical antipsychotic. Therefore, 6CM4 (D2 complex) and 6A93 (5-HT2A complex) were downloaded from the PDB database. Prior to docking studies, the ligands and receptors were prepared. The grid box containing the active residues of D2 and 5-HT2A is shown in Figure S3. Risperidone and clozapine were used as control drugs. Docking experiments were repeated with three ligands (two antipsychotics and the query compound) for both dopamine D2 and 5-HT2A receptors.

The docking conformations and interaction maps with the ligands for D2 (PDB ID: 6CM4) and 5-HT2A (PDB ID: 6A93) are shown in Figures 11 and 12, respectively. Table 10 shows a comprehensive interaction analysis between the ligands (THSB and the control drugs) and the receptors. The best binding scores of THSB were found to be -8.30 and -6.94 kcal/mol for D2 and 5-HT2A receptors, respectively. The remained docking parameters are shown in Table S6. For the D2 receptor, the binding energy of the ligand (-8.30 kcal/mol) was higher than that of clozapine (-8.07 kcal/mol) but lower than that of risperidone (-11.84

kcal/mol). THSB did not show superior antagonistic effect for the 5-HT2A receptor (binding energy: -6.94 kcal/mol) compared with the control drugs risperidone/-10.10 kcal/mol and clozapine/-11.47 kcal/mol. The control drugs continued to have the highest binding energies, which were higher than that of THSB.

In the D2-ligand interactions, the PHE189 residue was involved in the hydrophobic interactions for both THSB and risperidone. Residues TRP386, PHE389, and PHE 390 interacted together with risperidone and THSB and are involved in the π-stacking interactions. No common residues were found to be involved in the interactions between clozapine and THSB complexes

In the 5-HT2A-ligand interactions, the clozapine complex showed no common interactions with the THSB complex. Residues TRP 336 and PHE 340 were involved in π-stacking interactions, and these interactions were found to be common for risperidone and THSB complexes.

Table 10. *Docking results and comprehensive interaction parameters between ligands (query compound and antipsychotics) and receptors (D2R and 5-HT2A)*

	Dopamine D2 receptor (D2R)/6CM4		Serotonin 2A receptor (5-HT2A)/6A93	
	Docking score (kcal/mol)			
Query compound	**-8.30**		**-6.94**	
Clozapine	-8.07		-10.10	
Risperidone	-11.84		-11.47	
	Interaction analysis			
	Interacted residues	Distance (Å)	Interacted residues	Distance (Å)
Query compound				
Hydrogen bonds	SER193, HIS393	2.88, 3.12	-	-
Hydrophobic interactions	PHE189	3.33	-	-
Halogen bonds	TYR416	3.62	-	-
Π-stacking	TRP386, TRP386, PHE389, PHE390	4.99, 4.76, 4.56 4.89	TRP336, TRP336, PHE340	4.62, 4.74, 4.67
Clozapine				
Hydrogen bonds	TYR408	3.93	THR160, THR160, TYR370	3.43, 3.43, 3.60
Hydrophobic interactions	VAL91, LEU94, TRP100, TYR408 TRP413	3.97, 3.14, 3.16, 3.70, 3.98	VAL156, ILE163, PHE340	3.37, 3.76, 3.21
Halogen bonds	VAL91	2.99	-	-
Π-stacking	-	-	-	-
Salt bridges	ASP114	3.54	ASP155	3.10
Risperidone				
Hydrogen bonds	-	-	THR160, TYR370, TYR370	3.80, 3.96, 3.96
Hydrophobic interactions	PHE189, PHE382, TRP386, PHE389, PHE389, PHE390, PHE390, TYR408	3.91, 3.87, 3.49, 3.84, 3.60, 3.92, 3.93, 3.39	TRP151, VAL156, ILE163, LEU228, PHE243, PHE332, PHE339, VAL366, VAL366	3.20, 3.21, 3.28, 3.92, 2.60, 3.30, 3.73, 3.27, 3.77
Π-stacking	TRP386, TRP386, PHE389, PHE390	4.86, 4.88, 5.25, 4.95	TRP336, PHE340	5.35, 4.73
Salt bridges	ASP114	2.89	ASP155	2.92

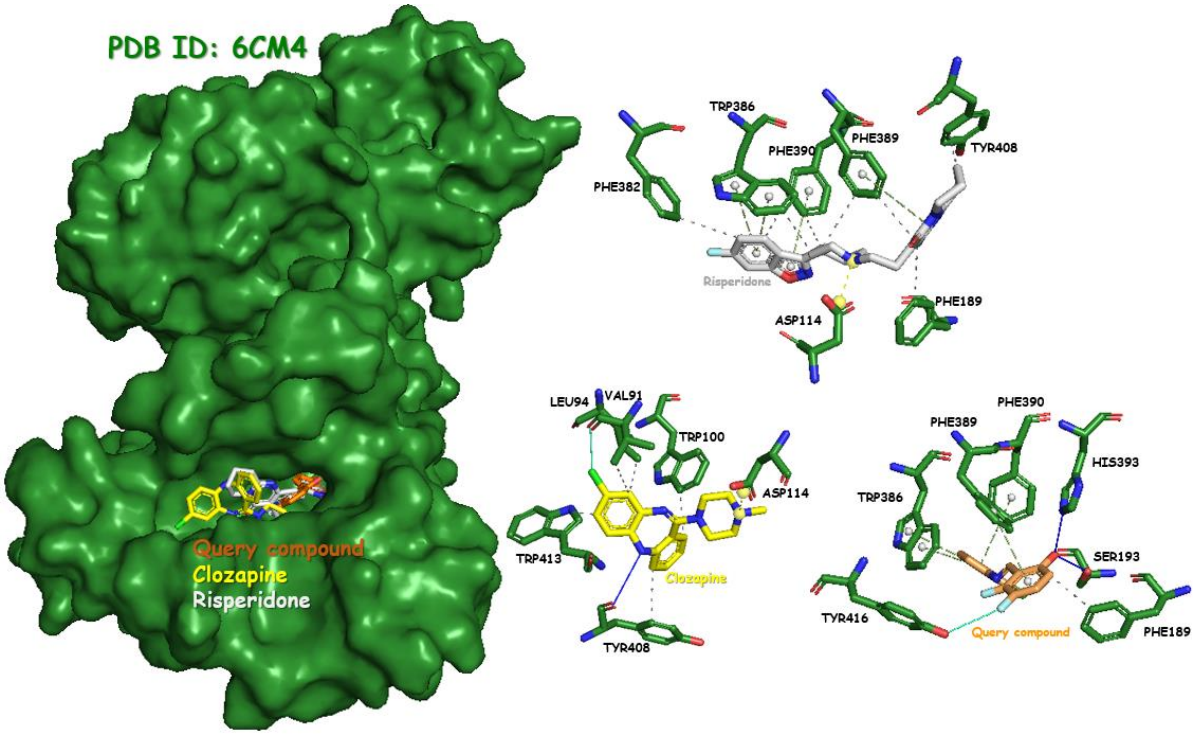

Figure 11. *Docking conformations of query compound and antipsychotics, clozapine and risperidone (left) with dopamine receptor D2; the interacted residues with ligands and secondary interaction types (right)*

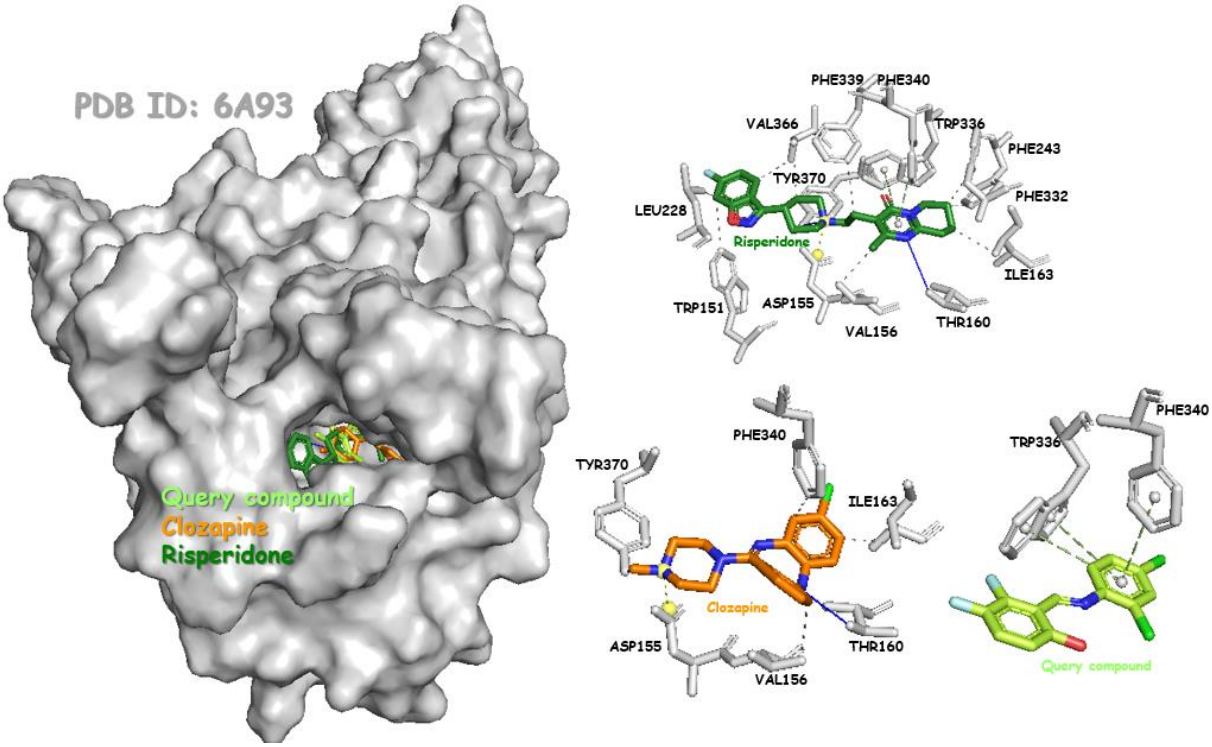

Figure 12. *Docking conformations of query compound and antipsychotics, clozapine and risperidone (left) with serotonin receptor 5-HT2A; the interacted residues with ligands and secondary interaction types (right)*

4. RESULTS

Finally, we reported a newly synthesized Schiff base compound substituted with two chlorine and two fluorine atoms ((THSB). We also revealed its crystallographic information and molecular properties, including secondary interactions, crystalline arrangement, surface analysis, electronic properties, chemical reactivity descriptors, and nonlinear optical properties. After the structural studies, *in silico* medicinal evaluations were performed because THSB contains pharmacologically active components such as fluorine and chlorine substituted with the aromatic ring, and imine groups. In this context, some physicochemical parameters affecting the pharmacokinetic effects were analyzed. The compound was evaluated based on ADME endpoints and some medicinal properties. To avoid random docking studies of THSB, comprehensive target identification studies were performed in drug or chemical library databases using based fingerprinting methods. Because of the moderately high similarity between THSB and the antipsychotics clozapine and loxapine, which are antagonists for the dopamine receptor (D2) and the serotonin receptor (5-HT2A), we selected these targets for molecular docking experiments. The 3D structures of the schizophrenia-related targets were obtained from the PDB database (complex with the antipsychotic risperidone). The results showed that the binding energy of the THSB-D2 complex was higher than that of the clozapine-D2 complex. For 5-HT2A ligand complexes, the control drugs remained the best rated compared with THSB.

CONFLICTS OF INTEREST

No conflict of interest was declared by the author.

REFERENCES

[1] El-Zahed, M.M., El-Sonbati, A.Z., Ajadain, F.M.S., Diab, M.A., and Abou-Dobara, M.I., "Synthesis, spectroscopic characterization, molecular docking and antimicrobial activity of Cu(II), Co(II), Ni(II), Mn(II) and Cd(II) complexes with a tetradentate ONNO donor Schiff base ligand", Inorganic Chemistry Communications, 152: 110710, (2023).

[2] Tada, K., Ikegaki, C., Fuse, Y., Tateishi, K., Sogawa, H., and Sanda, F., "Optically active polyaromatic Schiff base adopting stable secondary structures", Polymer, 268: 125703, (2023).

[3] Ibrahim, S.M., Saeed, A.M., Elmoneam, W.R.A., and Mostafa, M.A., "Synthesis and characterization of new Schiff base bearing bis(pyrano[3,2-c]quinolinone): Efficient cationic dye adsorption from aqueous solution", Journal of Molecular Structure, 1284: 135364, (2023).

[4] Sayed, F.N., Ashmawy, A.M., Saad, S.M., Omar, M.M., and Mohamed, G.G., "Design, spectroscopic characterization, DFT, molecular docking, and different applications: Anti-corrosion and antioxidant of novel metal complexes derived from ofloxacin-based Schiff base", Journal of Organometallic Chemistry, 993: 122698, (2023).

[5] Zhang, J., and Mu, Y., "A Schiff based p-phenylenediimine polymer as high capacity anode materials for stable lithium ion batteries", Electrochimica Acta, 450: 142276, (2023).

[6] Hernandes, M.Z., Cavalcanti, S.M., Moreira, D.R., de Azevedo Junior, W.F., and Leite, A.C., "Halogen atoms in the modern medicinal chemistry: hints for the drug design", Current Drug Targets, 11(3): 303-14, (2010).

[7] Inoue, M., Sumii, Y., and Shibata, N., "Contribution of Organofluorine Compounds to Pharmaceuticals", America Chemical Society Omega, 5(19): 10633-10640, (2020).

[8] Purser, S., Moore, P.R., Swallow, S., and Gouverneur, V., "Fluorine in medicinal chemistry",Chemical Society Reviews, 37(2): 320-330, (2008).

[9] Shah, P., and Westwell, A.D., "The role of fluorine in medicinal chemistry", Journal of Enzyme Inhibition and Medicinal Chemistry, 22(5): 527-540, (2007).

[10] Hagmann, W.K., "The Many Roles for Fluorine in Medicinal Chemistry", Journal of Medicinal Chemistry, 51(15): 4359-4369, (2008).

[11] Ge, H., Zhang, Y., Yang, Z., Qiang, K., Chen, C., Sun, L., Chen, M., and Zhang, J., "Chemical synthesis, microbial transformation and biological evaluation of tetrahydroprotoberberines as dopamine D1/D2 receptor ligands", Bioorganic & Medicinal Chemistry, 27(10): 2100-2111, (2019).

[12] Juza, R., Vojtechova, I., Stefkova-Mazochova, K., Dehaen, W., Petrasek, T., Prchal, L., Kobrlova, T., Janousek, J., Vlcek, P., Mezeiova, E., Svozil, D., Karasova, J.Z., Pejchal, J., Stark, H., Satala, G., Bojarski, A.J., Kubacka, M., Mogilski, S., Randakova, A., Musilek, K., Soukup, O., and Korabecny, J., "Novel D2/5-HT receptor modulators related to cariprazine with potential implication to schizophrenia treatment", European Journal of Medicinal Chemistry, 232: 114193, (2022).

[13] Ahmadi, R., Sepehri, B., Ghavami, R., and Irani, M., "Robust and predictive QSAR models for predicting the D2, 5-HT1A, and 5-HT2A inhibition activities of fused tricyclic heterocycle piperazine (piperidine) derivatives as atypical antipsychotic drugs", Journal of Molecular Structure, 1259: 132753, (2022).

[14] Venkataramaiah, C., Lakshmi Priya, B., and Rajendra, W., "Perturbations in the catecholamine metabolism and protective effect of "3-(3, 4-dimethoxy phenyl)-1-4(methoxy phenyl) prop-2-en-1-one" during ketamine-induced schizophrenia: an in vivo and in silico studies", Journal of Biomolecular Structure and Dynamics, 39(10): 3523-3532, (2021).

[15] Masaguer, C.F., Raviña, E., Fontenla, J.A., Brea, J., Tristán, H., and Loza, M.I., "Butyrophenone analogues in the carbazole series as potential atypical antipsychotics: synthesis and determination of affinities at D2, 5-HT2A, 5-HT2B and 5-HT2C receptors", European Journal of Medicinal Chemistry, 35(1): 83-95, (2000).

[16] Zhu, C., Li, X., Zhao, B., Peng, W., Li, W., and Fu, W., "Discovery of aryl-piperidine derivatives as potential antipsychotic agents using molecular hybridization strategy", European Journal of Medicinal Chemistry, 193: 112214, (2020).

[17] Aranda, R., Villalba, K., Raviña, E., Masaguer, C.F., Brea, J., Areias, F., Domínguez, E., Selent, J., López, L., Sanz, F., Pastor, M., and Loza, M.I., "Synthesis, Binding Affinity, and Molecular Docking Analysis of New Benzofuranone Derivatives as Potential Antipsychotics", Journal of Medicinal Chemistry, 51(19): 6085-6094, (2008).

[18] Sheldrick, G.M., "SHELXT - Integrated space-group and crystal-structure determination", Acta Crystallographica Section A: Foundations of Crystallography, 71(1): 3-8, (2015).

[19] Westrip, S.P., "PublCIF: Software for editing, validating and formatting crystallographic information files", Journal of Applied Crystallography, 43(4): 920-925, (2010).

[20] Macrae, C.F., Edgington, P.R., McCabe, P., Pidcock, E., Shields, G.P., Taylor, R., Towler, M., and Van De Streek, J., "Mercury: Visualization and analysis of crystal structures", Journal of Applied Crystallography, 39(3): 453-457, (2006).

[21] Spek, A., "checkCIF validation ALERTS: what they mean and how to respond", Acta Crystallographica Section E, 76(1): 1-11, (2020).

[22] Allen, F.H., Bellard, S., Brice, M.D., Cartwright, B.A., Doubleday, A., Higgs, H., Hummelink, T., Hummelink-Peters, B.G., Kennard, O., Motherwell, W.D.S., Rodgers, J.R., and Watson, D.G., "The Cambridge Crystallographic Data Centre: computer-based search, retrieval, analysis and display of information", Acta Crystallographica Section B, 35(10): 2331-2339, (1979).

[23] Becke, A.D., "Density-functional thermochemistry. III. The role of exact exchange", The Journal of Chemical Physics, 98(7): 5648-5652, (1993).

[24] Krishnan, R., Binkley, J.S., Seeger, R., and Pople, J.A., "Self-consistent molecular orbital methods. XX. A basis set for correlated wave functions", The Journal of Chemical Physics, 72(1): 650-654, (1980).

[25] Frisch, M., Trucks, G., Schlegel, H.B., Scuseria, G.E., Robb, M.A., Cheeseman, J.R., Scalmani, G., Barone, V., Mennucci, B., and Petersson, G., "gaussian 09, Revision d. 01, Gaussian", Inc., Wallingford CT, 201, (2009).

[26] Xiong, G., Wu, Z., Yi, J., Fu, L., Yang, Z., Hsieh, C., Yin, M., Zeng, X., Wu, C., Lu, A., Chen, X., Hou, T., and Cao, D., "ADMETlab 2.0: an integrated online platform for accurate and comprehensive predictions of ADMET properties", Nucleic Acids Research, 49(W1): W5-W14, (2021).

[27] Daina, A., Michielin, O., and Zoete, V., "SwissADME: a free web tool to evaluate pharmacokinetics, drug-likeness and medicinal chemistry friendliness of small molecules", Scientific Reports, 7(1): 42717, (2017).

[28] Banerjee, P., Eckert, A.O., Schrey, A.K., and Preissner, R., "ProTox-II: a webserver for the prediction of toxicity of chemicals", Nucleic Acids Research, 46(W1): W257-W263, (2018).

[29] Wang, L., Ma, C., Wipf, P., Liu, H., Su, W., and Xie, X.Q., "TargetHunter: an in silico target identification tool for predicting therapeutic potential of small organic molecules based on chemogenomic database", American Association of Pharmaceutical Sciences Journal, 15(2): 395-406, (2013).

[30] Awale, M., and Reymond, J.-L., "Polypharmacology Browser PPB2: Target Prediction Combining Nearest Neighbors with Machine Learning", Journal of Chemical Information and Modeling, 59(1): 10-17, (2019).

[31] Bragina, M.E., Daina, A., Perez, M.A.S., Michielin, O., and Zoete, V., "The SwissSimilarity 2021 Web Tool: Novel Chemical Libraries and Additional Methods for an Enhanced Ligand-Based Virtual Screening Experience", International Journal of Molecular Sciences, 23(2), (2022).

[32] Berman, H.M., Westbrook, J., Feng, Z., Gilliland, G., Bhat, T.N., Weissig, H., Shindyalov, I.N., and Bourne, P.E., "The Protein Data Bank", Nucleic Acids Research, 28(1): 235-242, (2000).

[33] Wang, S., Che, T., Levit, A., Shoichet, B.K., Wacker, D., and Roth, B.L., "Structure of the D2 dopamine receptor bound to the atypical antipsychotic drug risperidone", Nature, 555(7695): 269-273, (2018).

[34] Kimura, K.T., Asada, H., Inoue, A., Kadji, F.M.N., Im, D., Mori, C., Arakawa, T., Hirata, K., Nomura, Y., Nomura, N., Aoki, J., Iwata, S., and Shimamura, T., "Structures of the 5-HT2A receptor in complex with the antipsychotics risperidone and zotepine", Nature Structural & Molecular Biology, 26(2): 121-128, (2019).

[35] Morris, G.M., Huey, R., Lindstrom, W., Sanner, M.F., Belew, R.K., Goodsell, D.S., and Olson, A.J., "AutoDock4 and AutoDockTools4: Automated docking with selective receptor flexibility", Journal of computational chemistry, 30(16): 2785-2791, (2009).

[36] Salentin, S., Schreiber, S., Haupt, V.J., Adasme, M.F., and Schroeder, M., "PLIP: fully automated protein–ligand interaction profiler", Nucleic Acids Research, 43(W1): W443-W447, (2015).

[37] O'Boyle, N.M., Banck, M., James, C.A., Morley, C., Vandermeersch, T., and Hutchison, G.R., "Open Babel: An open chemical toolbox", Journal of cheminformatics, 3(1): 33, (2011).

[38] Đorović, J., Marković, Z., Petrović, Z.D., Simijonović, D., and Petrović, V.P., "Theoretical analysis of the experimental UV-Vis absorption spectra of some phenolic Schiff bases", Molecular Physics, 115(19): 2460-2468, (2017).

[39] Singh, M., Anthal, S., Srijana, P.J., Narayana, B., Sarojini, B.K., Likhitha, U., Kamal, and Kant, R., "Novel supramolecular co-crystal of 3-aminobenzoic acid with 4-acetyl-pyridine: Synthesis, X-ray structure, DFT and Hirshfeld surface analysis", Journal of Molecular Structure, 1262: 133061, (2022).

[40] Ethiraj, J., Ajin, R., Sankaranarayanan, R.K., Sekar, R., Veeman, D., Nanjan, M.J., and Varghese, J.J., "Crystallographic and computational investigations of structural properties in phenyl and methoxy-phenyl substituted 1,4 dihydropyridine derivatives", Journal of Molecular Structure, 1254: 132378, (2022).

[41] Turner, M., McKinnon, J., Wolff, S., Grimwood, D., Spackman, P., Jayatilaka, D., and Spackman, M., *CrystalExplorer17*, The University of Western Australia Australia. (2017).

[42] Singh, N., Fatima, A., Singh, M., kumar, M., Verma, I., Muthu, S., Siddiqui, N., and Javed, S., "Exploration of experimental, theoretical, Hirshfeld surface, molecular docking and electronic excitation studies of Menadione: A potent anti-cancer agent", Journal of Molecular Liquids, 351: 118670, (2022).

[43] Parte, M.K., Vishwakarma, P.K., Jaget, P.S., and Maurya, R.C., "Synthesis, spectral, FMOs and NLO properties based on DFT calculations of dioxidomolybdenum(VI) complex", Journal of Coordination Chemistry, 74(4-6): 584-597, (2021).

[44] Roy, R.K., Krishnamurti, S., Geerlings, P., and Pal, S., "Local Softness and Hardness Based Reactivity Descriptors for Predicting Intra- and Intermolecular Reactivity Sequences: Carbonyl Compounds", The Journal of Physical Chemistry A, 102(21): 3746-3755, (1998).

[45] Prasad, S., and Ojha, D.P., "Geometric structures, vibrational spectroscopic and global reactivity descriptors of nematogens containing strong polar group- A comparative analysis using DFT, HF and MP2 methods", Molecular Crystals and Liquid Crystals, 666(1): 12-28, (2018).

[46] Innasiraj, A., Anandhi, B., Gnanadeepam, Y., Das, N., Paularokiadoss, F., Ilavarasi, A.V., Sheela, C.D., Ampasala, D.R., and Jeyakumar, T.C., "Experimental and theoretical studies of novel Schiff base based on diammino benzophenone with formyl chromone – BPAMC", Journal of Molecular Structure, 1265: 133450, (2022).

[47] Mandal, D., Maity, R., Beg, H., Salgado-Morán, G., and Misra, A., "Computation of global reactivity descriptors and first hyper polarisability as a function of torsional angle of donor–acceptor substituted biphenyl ring system", Molecular Physics, 116(4): 515-525, (2018).

[48] Katariya, K.D., Nakum, K.J., and Hagar, M., "New thiophene chalcones with ester and Schiff base mesogenic Cores: Synthesis, mesomorphic behaviour and DFT investigation", Journal of Molecular Liquids, 359: 119296, (2022).

[49] Manivel, S., S Gangadharappa, B., Elangovan, N., Thomas, R., Abu Ali, O.A., and Saleh, D.I., "Schiff base (Z)-4-((furan-2-ylmethylene)amino) benzenesulfonamide: Synthesis, solvent interactions through hydrogen bond, structural and spectral properties, quantum chemical modeling and biological studies", Journal of Molecular Liquids, 350: 118531, (2022).

[50] Meenukutty, M.S., Mohan, A.P., Vidya, V.G., and Viju Kumar, V.G., "Synthesis, characterization, DFT analysis and docking studies of a novel Schiff base using 5-bromo salicylaldehyde and β-alanine", Heliyon, 8(6): e09600, (2022).

[51] Shobana, D., Sudha, S., Ramarajan, D., and Dimić, D., "Synthesis, crystal structure, spectral characterization and Hirshfeld surface analysis of (E)-N′-(3-ethoxy-4-hydroxybenzylidene)-4-fluorobenzohydrazide single-crystal – a novel NLO active material", Journal of Molecular Structure, 1250: 131856, (2022).

[52] Guerroudj, A.R., Boukabcha, N., Benmohammed, A., Dege, N., Belkafouf, N.E.H., Khelloul, N., Djafri, A., and Chouaih, A., "Synthesis, crystal structure, vibrational spectral investigation, intermolecular interactions, chemical reactivity, NLO properties and molecular docking analysis on (E)-N-(4-nitrobenzylidene)-3-chlorobenzenamine: A combined experimental and theoretical study", Journal of Molecular Structure, 1240: 130589, (2021).

[53] Solo, P., and Arockia doss, M., "Synthesis, Single-Crystal XRD, Spectral and Computational Analysis of 2-(3,4-Dimethoxyphenyl)-1H-Phenanthro[9,10-d] Imidazole as Electron-Transport and NLO Material", Polycyclic Aromatic Compounds, 1-14, (2022).

[54] Jothi, A.I., Paul, M.W.B., and Alexander, V., "A comparative molecular structure – NLO activity study of ortho-bridged dibenzaldehydes: Synthesis, crystal structure, SHG, and DFT studies", Journal of Molecular Structure, 1250: 131776, (2022).

[55] van de Waterbeemd, H., and Gifford, E., "ADMET in silico modelling: towards prediction paradise? ", Nature Reviews Drug Discovery, 2(3): 192-204, (2003).

[56] Venkatraman, V., "FP-ADMET: a compendium of fingerprint-based ADMET prediction models", Journal of Cheminformatics, 13(1): 75, (2021).

[57] Lipinski, C.A., Lombardo, F., Dominy, B.W., and Feeney, P.J., "Experimental and computational approaches to estimate solubility and permeability in drug discovery and development settings", Advanced Drug Delivery Reviews, 23(1): 3-25, (1997).

[58] Hughes, J.D., Blagg, J., Price, D.A., Bailey, S., DeCrescenzo, G.A., Devraj, R.V., Ellsworth, E., Fobian, Y.M., Gibbs, M.E., Gilles, R.W., Greene, N., Huang, E., Krieger-Burke, T., Loesel, J., Wager, T., Whiteley, L., and Zhang, Y., "Physiochemical drug properties associated with in vivo toxicological outcomes", Bioorganic & Medicinal Chemistry Letters, 18(17): 4872-4875, (2008).

[59] Gleeson, M.P., "Generation of a Set of Simple, Interpretable ADMET Rules of Thumb", Journal of Medicinal Chemistry, 51(4): 817-834, (2008).

[60] Farah, A., "Atypicality of atypical antipsychotics", Prim Care Companion J Clin Psychiatry, 7(6): 268-74, (2005).

[61] Shi, L., Fang, R.Q., Zhu, Z.W., Yang, Y., Cheng, K., Zhong, W.Q., and Zhu, H.L., "Design and synthesis of potent inhibitors of beta-ketoacyl-acyl carrier protein synthase III (FabH) as potential antibacterial agents", European Journal of Medicinal Chemistry, 45(9): 4358-64, (2010).

[62] Misra, S., Pandeya, K.B., Tiwari, A.K., Ali, A.Z., Saradamani, T., Agawane, S.B., and Madhusudana, K., "Antihyperglycemic, α-glucosidase inhibitory and DPPH free radical scavenging activity of 5-bromosalicylaldehyde and schiff bases", Medicinal Chemistry Research, 20(9): 1431-1437, (2011).

[63] Chen, Y., Wen, D., Huang, Z., Huang, M., Luo, Y., Liu, B., Lu, H., Wu, Y., Peng, Y., and Zhang, J., "2-(4-Chlorophenyl)-2-oxoethyl 4-benzamidobenzoate derivatives, a novel class of SENP1 inhibitors: Virtual screening, synthesis and biological evaluation", Bioorganic and Medicinal Chemistry Letters, 22(22): 6867-70, (2012).

[64] Popovic, D., Nuss, P., and Vieta, E., "Revisiting loxapine: a systematic review", Annals of General Psychiatry, 14: 15, (2015).